MARTIN MARIETTA ENERGY SYSTEMS LIBRARIES

3 4456 0347637 0

ORNL/TM-11378

ornl

OAK RIDGE NATIONAL LABORATORY

MARTIN MARIETTA

Selection of Support Structure Materials for Irradiation Experiments in the HFIR at Temperatures Up to 500°C

K. Farrell and A. W. Longest

OAK RIDGE NATIONAL LABORATORY
CENTRAL RESEARCH LIBRARY
CIRCULATION SECTION
4500N ROOM 175
LIBRARY LOAN COPY
DO NOT TRANSFER TO ANOTHER PERSON
If you wish someone else to see this report, send in name with report and the library will arrange a loan.

OPERATED BY
MARTIN MARIETTA ENERGY SYSTEMS, INC.
FOR THE UNITED STATES
DEPARTMENT OF ENERGY

This report has been reproduced directly from the best available copy.

Available to DOE and DOE contractors from the Office of Scientific and Technical Information, P.O. Box 62, Oak Ridge, TN 37831; prices available from (615) 576-8401, FTS 626-8401.

Available to the public from the National Technical Information Service, U.S. Department of Commerce, 5285 Port Royal Rd., Springfield, VA 22161.
NTIS price codes—Printed Copy: A03 Microfiche A01

This report was prepared as an account of work sponsored by an agency of the United States Government. Neither the United States Government nor any agency thereof, nor any of their employees, makes any warranty, express or implied, or assumes any legal liability or responsibility for the accuracy, completeness, or usefulness of any information, apparatus, product, or process disclosed, or represents that its use would not infringe privately owned rights. Reference herein to any specific commercial product, process, or service by trade name, trademark, manufacturer, or otherwise, does not necessarily constitute or imply its endorsement, recommendation, or favoring by the United States Government or any agency thereof. The views and opinions of authors expressed herein do not necessarily state or reflect those of the United States Government or any agency thereof.

ORNL/TM-11378
Distribution
Category UC-404

Metals and Ceramics Division

SELECTION OF SUPPORT STRUCTURE MATERIALS FOR IRRADIATION EXPERIMENTS IN THE HFIR AT TEMPERATURES UP TO 500°C

K. Farrell and A. W. Longest

Date Published: January 1990

NOTICE: This document contains information of a preliminary nature. It is subject to revision or correction and therefore does not represent a final report.

Prepared for the
DOE Division of Materials Sciences
KC 02 01 04 0

Prepared by the
OAK RIDGE NATIONAL LABORATORY
Oak Ridge, Tennessee 37831-6285
operated by
MARTIN MARIETTA ENERGY SYSTEMS, INC.
for the
U.S. DEPARTMENT OF ENERGY
under contract DE-AC05-84OR21400

MARTIN MARIETTA ENERGY SYSTEMS LIBRARIES

3 4456 0347637 0

CONTENTS

LIST OF FIGURES v

LIST OF TABLES vii

ABSTRACT 1

INTRODUCTION 1

IRRADIATION PROGRAM 2

CAPSULE DESIGN REQUIREMENTS 2

CAPSULE MATERIALS REQUIREMENTS AND SELECTION 8

EVALUATION OF AN ALTERNATIVE OXIDE-DISPERSION-HARDENED ALUMINUM ALLOY 19

ACKNOWLEDGMENTS 27

REFERENCES 27

LIST OF FIGURES

		Page
Fig. 1.	New experimental facilities in the HFIR	3
Fig. 2.	Magnetic fusion energy materials specimens	4
Fig. 3.	Lower half of the HFIR-MFE-330J-1 capsule	6
Fig. 4.	Calculated radial temperature profile for the HFIR-MFE-330J-1 capsule	7
Fig. 5.	Thermal conductivities of candidate materials as functions of temperature	10
Fig. 6.	Temperature dependencies of tensile yield strengths of candidate materials	11
Fig. 7.	Stress-rupture properties of SAP alloys M583 and SAP930	14
Fig. 8.	Creep-rupture lives of 6061-T6 alloy at 50 to 150°C, before and after irradiation	15
Fig. 9.	Swelling in aluminum alloys during neutron irradiation at 55°C	17
Fig. 10.	Temperature dependencies of tensile properties of aluminum alloy XAP002 in longitudinal and transverse directions	22
Fig. 11.	Temperature dependencies of tensile properties of aluminum alloy in longitudinal and transverse directions	23
Fig. 12.	Temperature dependencies of tensile properties of aluminum alloy DISPAL 0.2 in longitudinal and transverse directions	24
Fig. 13.	Typical microstructures of (*a*) XAP002 and (*b*) DISPAL 0.2 alloys, showing finer particles (arrowed) in the DISPAL 0.2 alloy	26

LIST OF TABLES

Page

Table 1. Physical and nuclear properties of candidate structural materials 9

Table 2. Chemical analyses of test bars 21

Table 3. Effects of annealing DISPAL 0.2 for 24 h at 500°C 25

SELECTION OF SUPPORT STRUCTURE MATERIALS FOR IRRADIATION EXPERIMENTS IN THE HFIR AT TEMPERATURES UP TO 500°C*

K. Farrell and A. W. Longest

ABSTRACT

The key factor in the design of capsules for irradiation of test specimens in the High Flux Isotope Reactor at preselected temperatures up to 500°C utilizing nuclear heating is a narrow gas-filled gap which surrounds the specimens and controls the transfer of heat from the specimens through the wall of a containment tube to the reactor cooling water. Maintenance of this gap to close tolerances is dependent on the characteristics of the materials used to support the specimens and isolate them from the water. These support structure materials must have low nuclear heating rates, high thermal conductivities, and good dimensional stabilities under irradiation. These conditions are satisfied by certain aluminum alloys. One of these alloys, a powder metallurgy product containing a fine dispersion of aluminum oxide, is no longer manufactured. A new alloy of this type, with the trade name DISPAL, is determined to be a suitable substitute.

INTRODUCTION

A series of irradiations is being conducted in the High Flux Isotope Reactor (HFIR) under a collaborative U.S.-Japanese test program. The objective is to determine the responses of various stainless steels to the combined effects of displacement damage and high levels of nuclear-generated helium at specified temperatures in the range of 60 to 400°C, and possibly to 500°C. Heating is derived from gamma rays and to a lesser extent neutron bombardment, and the chosen temperatures are maintained by balancing the rate of generation of this nuclear heat against controlled transfer of the heat to the cooling water of the reactor. To achieve this

*Research sponsored by the Division of Materials Sciences, U.S. Department of Energy under Contract DE-AC05-84OR21400 with Martin Marietta Energy Systems, Inc.

balance, the design of the irradiation capsule supporting the test specimens and the choice of materials for the construction of the capsules are critical. This report outlines the required design and materials characteristics. The support materials used in the first capsules are described, and the results of qualification tests made on a substitute material, a mechanically alloyed aluminum alloy with the trade name DISPAL, are presented.

IRRADIATION PROGRAM

The irradiations are being carried out in the new irradiation facilities in the removable portion of the beryllium reflector of the HFIR core, named "removable beryllium star" (RB*) sites,[1] as shown in Fig. 1. The experiments are designated HFIR-MFE-RB* to signify that the specimens belong to the Magnetic Fusion Energy (MFE) first-wall materials program. The first four HFIR-MFE-RB* capsules will irradiate MFE materials specimens at temperatures of 60, 200, 330, and 400°C. Later capsules may run at 500°C. These experiments provide for removal, examination, and reencapsulation of the MFE specimens at intermediate exposure levels en route to a target exposure level of 30 displacements per atom (dpa). Each capsule will hold between 200 and 300 miniature mechanical property specimens of austenitic and martensitic/ferritic stainless steels. The shapes and sizes of these specimens are illustrated in Fig. 2.

CAPSULE DESIGN REQUIREMENTS

Heat generation rates are high in the HFIR-RB* positions, up to 15 watts per gram of material. For irradiations at 60°C (±10°), all of the nuclear heat generated in the specimens and in the capsule materials must be transferred efficiently to the reactor cooling water, which enters the reactor at 49°C. This is effected simply by holding the specimens loosely in open slots and holes in a cylindrical 6061-T6 aluminum holder that is in direct contact with the flowing cooling water.

For irradiation at higher temperatures, the heat flux to the cooling water must be retarded enough to retain sufficient heat to maintain the

ORNL-DWG 85-18469R2

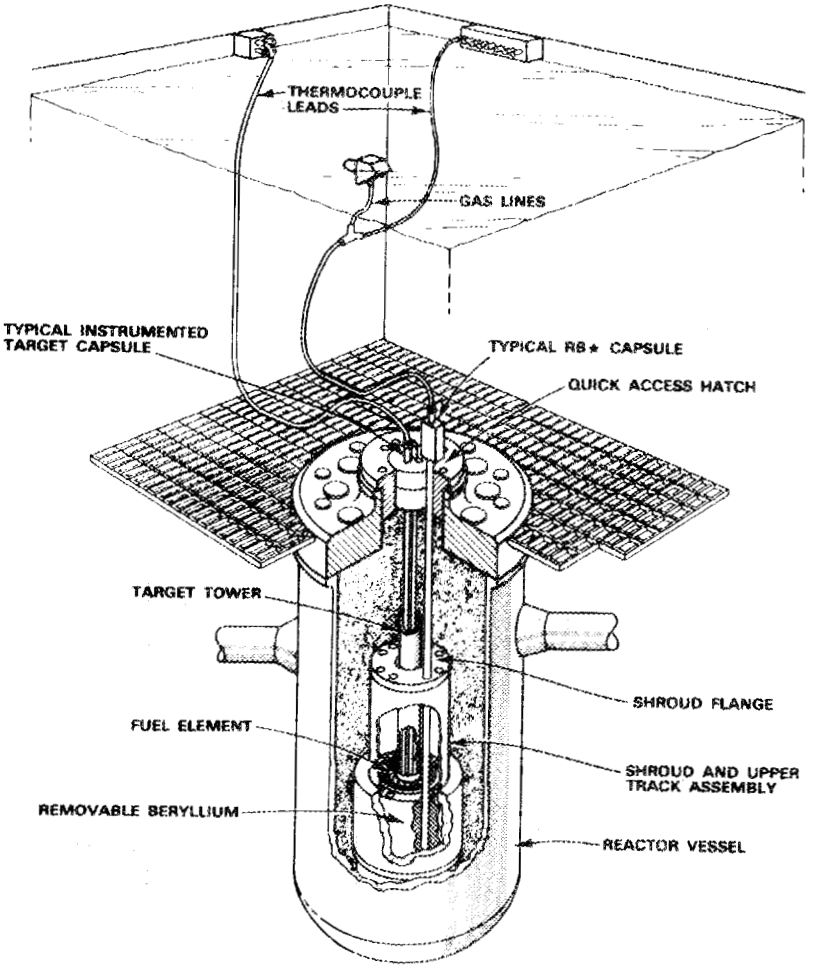

Fig. 1. New experimental facilities in the HFIR.

specimens at their designated temperatures. This involves the use of a higher-resistance heat transfer path. The specimens in their cylindrical holder are sealed off from the water by a containment tube. This tube is separated from the holder by a symmetric gas-filled gap, which impedes heat flow to the tube wall and thence to the water. The temperature of the specimen holder is controlled by the width of the gap and the thermal conductivity of the gas in the gap. The tube, which is in contact with the reactor cooling water, and the specimen holder should have good thermal conductivities.

ORNL-DWG 87-15260

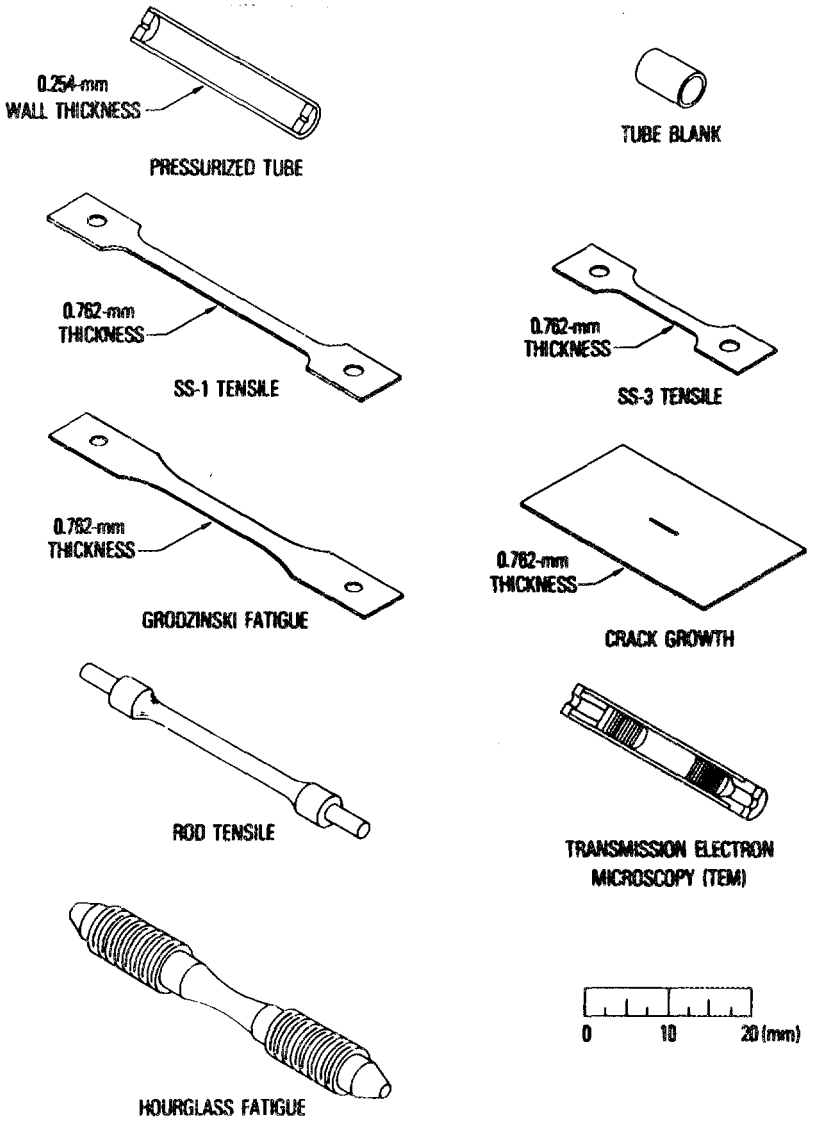

Fig. 2. Magnetic fusion energy materials specimens.

The width of the gas gap varies with the desired irradiation temperature and must be maintained within close tolerances for each temperature. Since the holder contains open slots to house many of the specimens, achieving a uniform gap between the holder and the tube wall is impractical. This problem is overcome by slipping a close-fitting sleeve over the holder and setting the symmetric gas gap between the sleeve and

the water-cooled tube wall. The sleeve also serves two other purposes: it retains the specimens in their slots and provides a barrier between the gas in the gap and another gas (pure helium) which flows gently through the specimen slots and holes in the holder. This holder gas has nothing to do with the gas in the temperature-control gap. Its function is to ensure rapid transfer of heat from the specimens to the holder and the sleeve; it does not provide significant cooling. The gas in the holder cavities is required to have as high a thermal conductivity as possible, whereas the gas in the control gap needs to have a lower (and variable) conductivity to permit manipulation of the gap's resistance to heat flow to the exterior cooling water.

The 330°C capsule design[2] is typical of the elevated temperature capsules. This capsule, designated HFIR-MFE-330J-1, is shown in Fig. 3. The various specimens are arranged in slots and holes in a solid, cylindrical aluminum alloy specimen holder; those in slots are held tightly against the holder by springs of a nickel alloy, Inconel X750. The specimens and holder are enclosed by a tight-fitting sleeve of aluminum alloy. The specimen slots and holes are interconnected so that the helium atmosphere of the holder can trickle through them. Twenty-one type K thermocouples are located throughout the specimen holder to provide continuous measurement of the temperature distribution. Surrounding the holder sleeve is the containment tube, 38.1-mm OD and 3-mm wall thickness, made from aluminum alloy. The symmetrical temperature-control gas gap between the outer surface of the holder sleeve and the inner surface of the containment tube is 0.089 mm (0.0035 in.) wide at the operating temperature of 330°C and must be held to tolerance for control of temperature in the holder. Under the 330°C design operating conditions, a change in the gap width of only 0.01 mm (0.0004 in.) will alter the temperature of the specimens and holder by approximately 25°.

The 330°C capsule will be operated at an internal gas pressure of 207 kPa gage (30 psig) and cooled with reactor coolant water, at an inlet temperature of 49°C, flowing downward over the containment tube surface. The specimen-holder temperature, monitored by the thermocouples, will be controlled by adjusting the composition and hence the thermal conductivity of a flowing mixture of helium and neon in the narrow control gas gap.

ORNL-DWG 87-15259

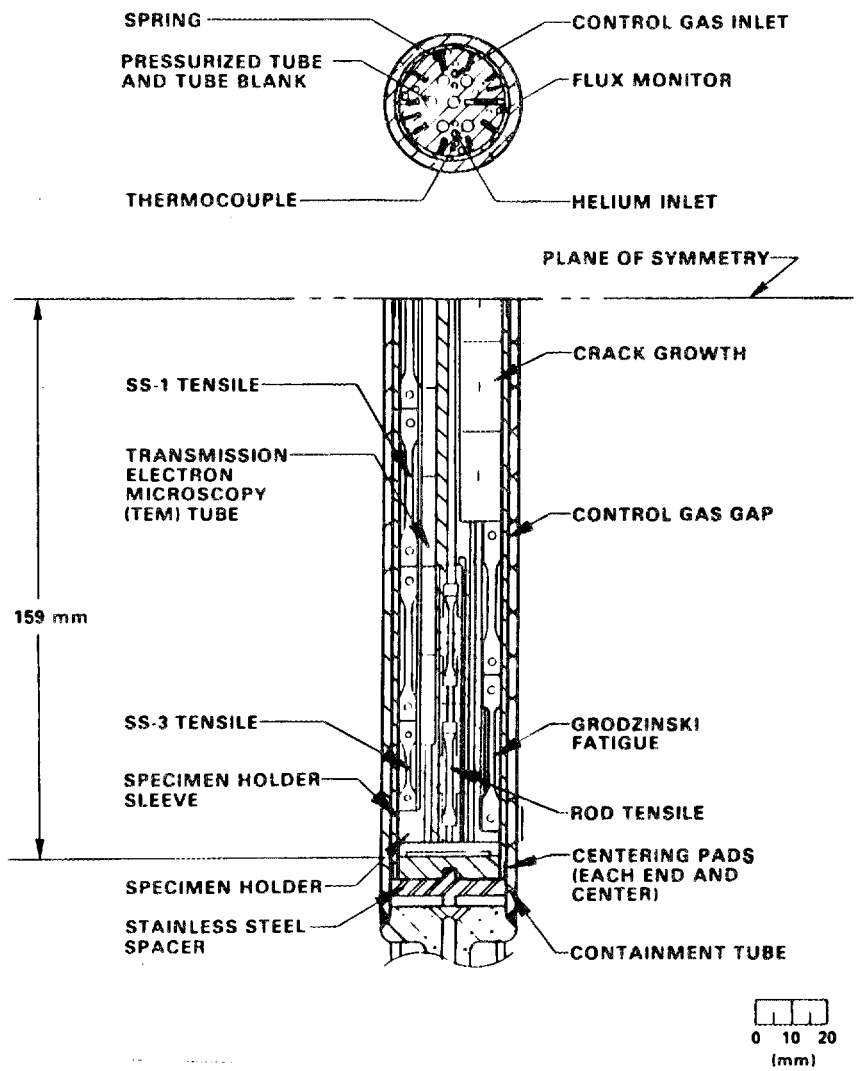

Fig. 3. Lower half of the HFIR-MFE-330J-1 capsule.

The normal flow rate of the control gas mixture will be ~0.6 cm^3/s. Calculated temperature distributions[2] in the 330°C capsule indicate that specimen temperatures can be maintained within 25°C of 330°C, which satisfies the temperature criterion for these experiments. A typical radial temperature profile calculated by a one-dimensional heat transfer code is given in Fig. 4. In this calculation, an average nuclear heating rate of 10.9 W/g was used. As is evident in this figure, most of the temperature

ORNL-DWG 88-15088

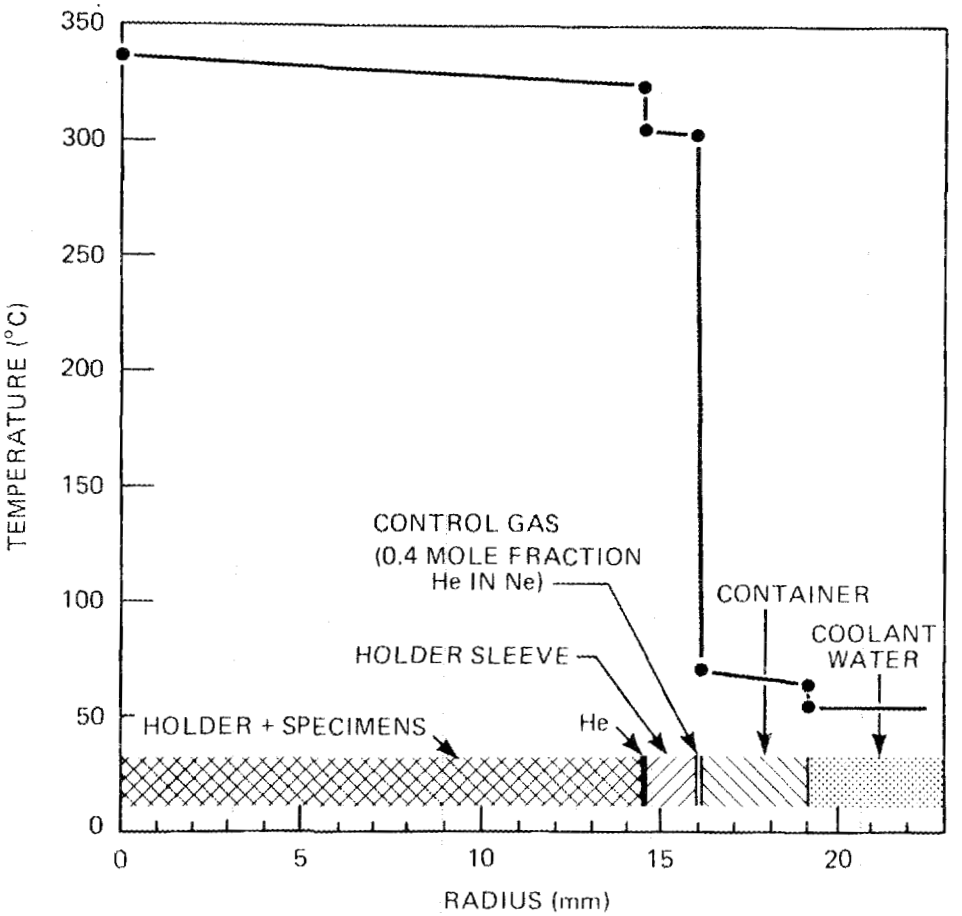

Fig. 4. Calculated radial temperature profile for the HFIR-MFE-330J-1 capsule.

drop is across the control gas gap (for maximum temperature control capability), while the drops across the specimen holder plus specimens (homogenized) and container wall regions are small. At these design operating conditions, thermal conductivities of the helium purge gas and control gas (0.4 mole fraction He in Ne) are 0.225 and 0.102 W/(m·K), respectively. Calculations of the range of nuclear heating rates that can be accommodated by varying the composition of the temperature-control gas mixture between pure helium and pure neon indicated 7.0 W/g for pure neon to 18.0 W/g for pure helium.

CAPSULE MATERIALS REQUIREMENTS AND SELECTION

There are four critical parameters in the design of a successful capsule for these elevated temperature irradiations. The first is the mass of the capsule (specimens + holder + sleeve + container), which determines the amount of nuclear heat generated. The second is the width of the gas gap, which must remain constant at the operating temperature. The third is high thermal conductivities of holder and tube materials for homogenization of heat inside the capsule and for conducting the heat rapidly to the cooling water once it has crossed the gas gap. The fourth is the properties of the gas used in the gap.

The heat transfer gas must neither react chemically with the capsule materials nor diffuse into or through them. Also, for easy disposal, it is desirable that the gas not be activated by neutron bombardment. Its heat capacity is not an important consideration, since relatively little heat will be removed from the capsule by the slow-rate, once-through flow of gas in the gap. Most of the heat transfer is via conductance across the gap. The thermal conductivity of the gas should be variable in a controlled manner to permit temperature adjustment during irradiation. The noble gases are the obvious choices. But not all are equally suitable. Argon, for example, becomes activated to ^{41}Ar, which emits gamma rays and poses a handling hazard. Helium has the highest thermal conductivity, and when it is mixed with neon, the conductivity of the mixture can be varied by adjusting the helium to neon ratio during irradiation to compensate for changes in heat generation rate.

The criteria for the capsule materials are specified largely by the needs to minimize the quantity of heat generated and to ensure appropriate transfer of the heat to the reactor coolant. These conditions are determined by the physical properties of the materials and by their radiation responses. In general, materials selected for the irradiation capsule should have the following characteristics:

1. low nuclear heat generation rate,
2. good dimensional stability at the planned irradiation conditions,

3. high thermal conductivity,
4. compatibility with water and with other materials in the capsule and reactor,
5. good machinability,
6. low neutron absorption for neutron economy, and
7. low residual radioactivity (a desirable characteristic for disposal of used capsules).

Important physical and nuclear properties of candidate structural materials from a variety of sources[3-14] are given in Table 1.

Table 1. Physical and nuclear properties of candidate structural materials

Material	Density (Mg/m^3)	Melting point (°C)	Thermal conductivity at 20°C [W/(m·K)]	Absorption cross-section for thermal (2200 m/s) neutrons (barns)
Elements				
Mg	1.74	650	170	0.063
Be	1.85	1283	159	0.0095
Al	2.70	660	209	0.23
Ti	4.51	1660	18	~6.0
Zr	6.50	1845	23.9	0.18
Fe	7.87	1539	75.3	2.53
Cu	8.90	1083	395	3.85
Ni	8.91	1455	92.1	4.6
Alloys				
Magnox Al80	~1.8	647	117	Similar to Mg
6061-T6 Al	2.70	629–650	217	Similar to Al
SAP XAP002	2.74	660	170	0.22
304L stainless steel	7.9	1400–1455	16[a]	
Inconel	8.51	1390–1430	15[a]	

[a]At 100°C.

Thermal conductivities and tensile yield strengths (from refs. 7–14) are plotted as functions of temperature for several elements and alloys of interest in Figs. 5 and 6, respectively. It will be shown shortly that a high level of mechanical strength is not an important criterion in these

ORNL-DWG 88-10841R

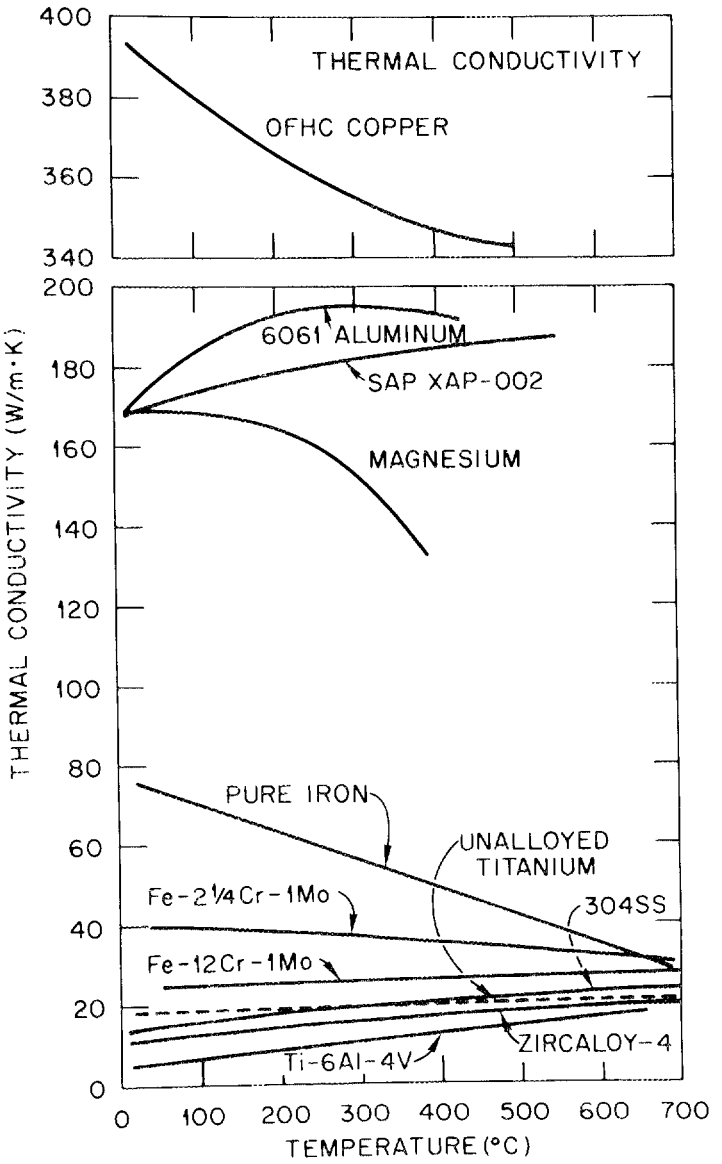

Fig. 5. Thermal conductivities of candidate materials as functions of temperature.

ORNL-DWG 88-10842R

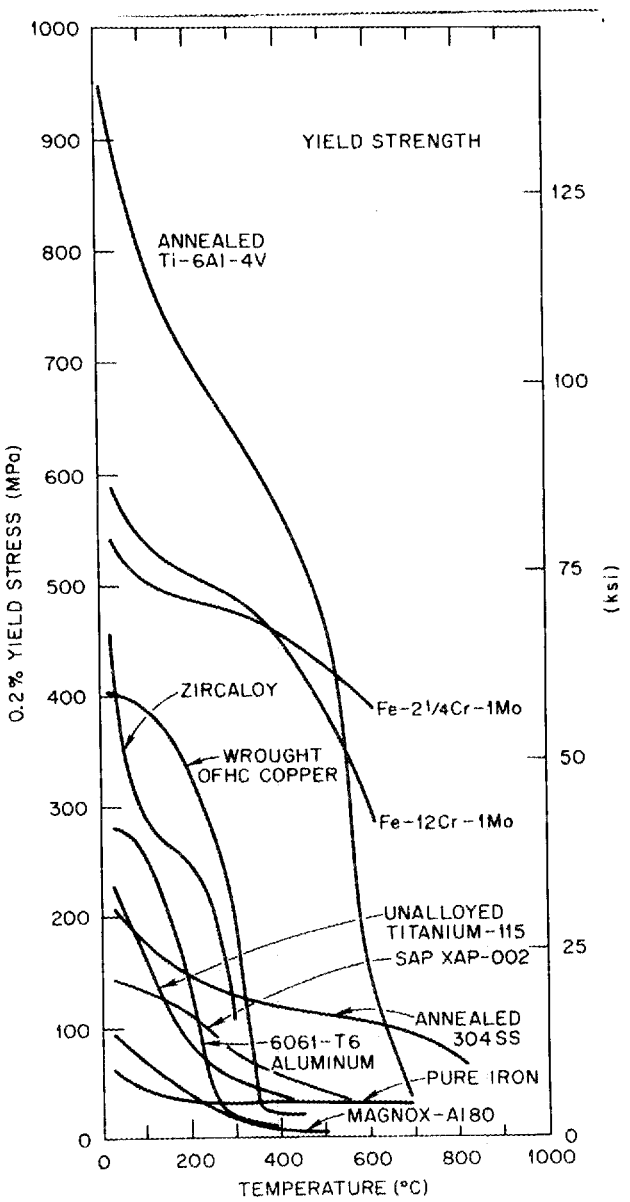

Fig. 6. Temperature dependencies of tensile yield strengths of candidate materials.

experiments. Nuclear heating rates and thermal conductivities are important. The nuclear heating rate of a material from gamma rays is approximately proportional to its physical density.[6] Therefore, the

lightweight materials – Mg, Be, and Al – will generate the least nuclear heat. These materials have good thermal conductivities, too. Other candidate materials fare poorly in these combined properties. Oxygen-free, high-conductivity-grade copper, with the highest thermal conductivity, has a high nuclear heating rate; it is also undesirable for use in the HFIR because copper ions in the cooling water may accelerate corrosion of aluminum components of the HFIR. Steels and Zircaloy have high heating rates and low thermal conductivities. Titanium offers low conductivity and poor neutron economy. Since the high strengths of these latter materials are not of benefit to these experiments, we can eliminate them from further consideration. The field of contenders is thus reduced to Mg, Be, and Al. We shall soon see that unacceptable radiation responses rule out Mg and Be, leaving Al as the preferred material. Despite its low density, an aluminum holder still makes a considerable contribution to the heat load. To accommodate the large number of test specimens, a relatively large volume of support material is required, e.g., a 32-mm-diam bar including sleeve, which provides about 75% of the heat load in the capsule.

The width of the gas gap at temperature must not change substantially during irradiation. Small changes, detected by perturbations in the recorded temperatures of the specimen holder, can be compensated for during the experiments by adjusting the composition (conductivity) of the gas in the gap. Changes greater than about 25% may not be tolerable. A 25% leeway may seem large, but in fact the actual dimensional changes are very small because the gas gaps are small, especially for the 200°C irradiation. The cylindrical gas gap for the 200°C capsule is only 0.029 mm wide with an outer diameter of 32.2 mm. A 25% change in the width of this gap is a mere 0.00725 mm, or 0.045% of the internal radius of the container tube. Factors that might conceivably affect the stability of these small gaps are creep flow and radiation-induced swelling.

Alteration of the gas gaps by creep flow of the support materials is not a problem in these irradiations. The stresses on the system are low, and as an extra safeguard, creep-resistant materials are used. The stress on the holder sleeve, assuming it bears the full load of the specimens plus holder plus the weight of a stainless steel radiation shield plug immediately above the radiation zone, is only about 0.15 MPa (22.5 psi).

Although this stress is minor, it should be remembered that most aluminum alloys lose their strength sharply at temperatures of about 100°C and are not recommended for prolonged use under load at temperatures above about 200°C. An exception is the class of powder metallurgy alloys containing a mechanically entrained dispersion of fine, stable aluminum oxide particles[12-14] known generically as sintered aluminum products (SAP). SAP alloys are labelled with various manufacturers' trade names. Those with Al_2O_3 contents in the range of 6 to 8 wt % have names like XAP002, M583, and SAP930, depending on their source. The alloy XAP002, which was used to make the holder and sleeve for the 330°C capsule, was manufactured many years ago by ALCOA Corporation using SAP930 (7% Al_2O_3) powders provided by Montecatini-Edison StA, Italy. SAP alloys have good resistance to creep at temperatures up to 500°C, as shown for the alloys M583 and SAP930 in Fig. 7.[13] At 500°C, they offer a 1000-h rupture life at stresses as high as 34 MPa (5 ksi). Thus, the use of alloy XAP002 for the holder block and sleeve obviates any question of creep deformation occurring at the low stresses on the capsule support materials at all temperatures up to 500°C. The containment tube operates at only about 60°C. The external stress on the tube from the pressure of the reactor coolant water is about 3 MPa (440 psi), which produces a compressive stress in the tube wall of about 21 MPa (3 ksi). These containment tube conditions of temperature and stress do not require the use of a special alloy like SAP. They can be handled adequately by a more common aluminum alloy, 6061-T6, from which many of the components of the HFIR are built and which has the best-established irradiation-response pattern for the HFIR conditions. The 6061 alloy is a heat-treatable material containing 1% Mg and 0.5% Si, which in the quenched-and-tempered condition (T6) has a 10,000-h creep strength exceeding 250 MPa (about 36 ksi) at 60°C, as illustrated in Fig. 8.[15] Irradiation raises the creep strength, giving a greater margin of creep resistance.

Radiation-induced swelling poses a greater threat to the gas gaps, particularly if the swelling is unequal in different components of the capsule and especially at the lower operating temperatures where the gas gaps are narrower. If the tube swells and the holder does not swell, the gap will enlarge. In the 200°C capsule a 25% increase in the width of the gap will ensue from just 0.13% swelling of the containment tube. In

ORNL-DWG 89-18640

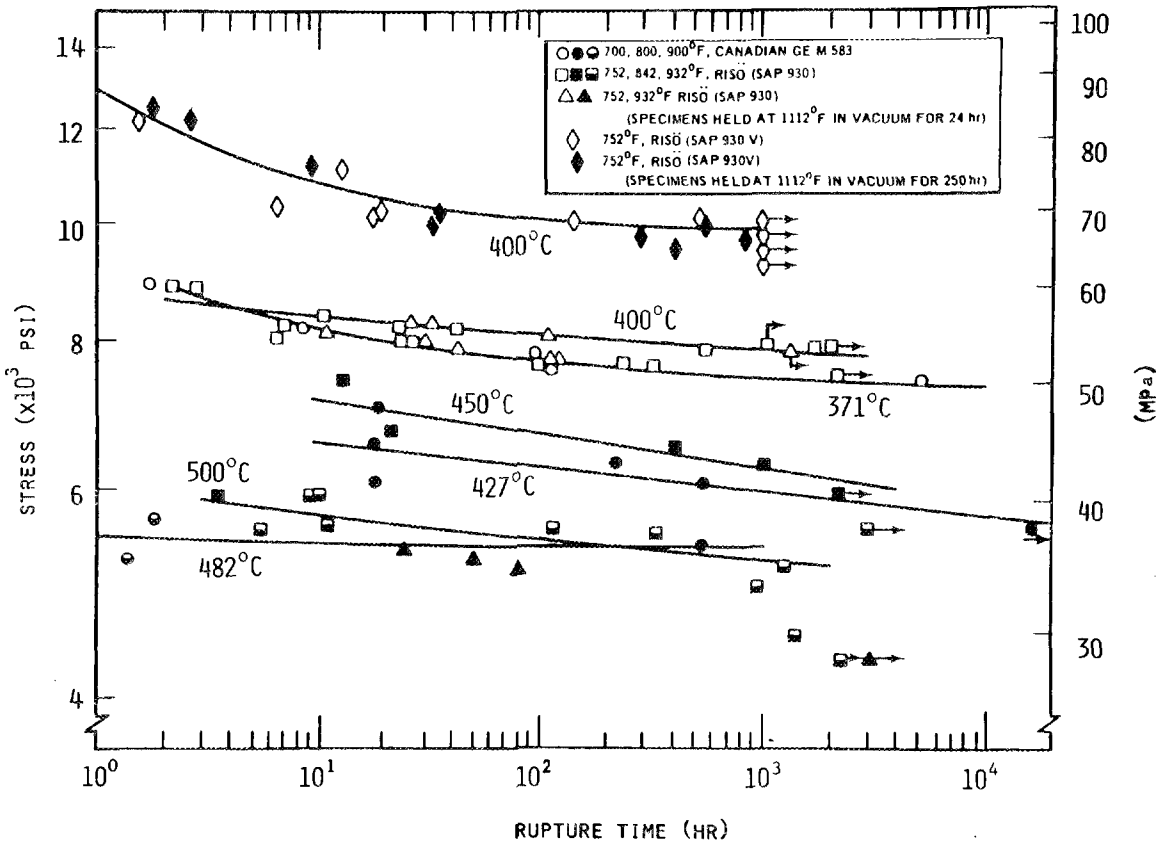

Fig. 7. Stress-rupture properties of SAP alloys M583 and SAP930.

aluminum, swelling arises from three different sources: precipitates of transmutation-produced silicon, voids, and gas bubbles. The different temperature dependencies of these phenomena may lead to unequal degrees of swelling in different components of the capsule.

Swelling from transmutation-produced silicon is a result of the reaction of thermal neutrons with aluminum nuclei. The reaction cross-section is 0.23 barns for 2200 m/s neutrons, and about 0.1 wt % Si is generated for every thermal neutron fluence of 4×10^{25} n/m². Silicon is essentially insoluble in aluminum, and the transmutation-produced silicon develops into precipitates of silicon that are less dense than aluminum (2.3 Mg/m³ vs 2.7 Mg/m³) and take up more space. Each 1% silicon causes about 0.16% swelling. The fluxes of thermal neutrons in the RB* positions are large. But in these U.S.-Japanese experiments, hafnium liners in the

ORNL-DWG 89M-7070

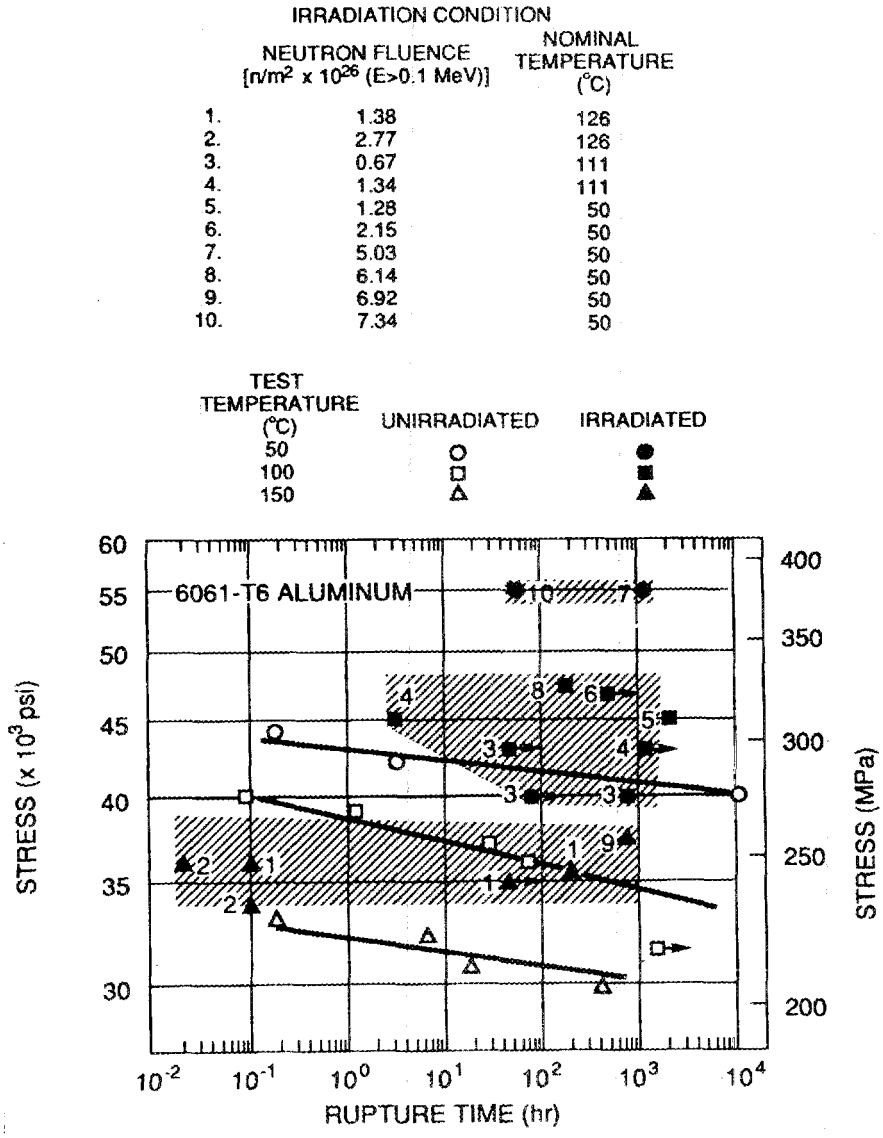

Fig. 8. Creep-rupture lives of 6061-T6 alloy at 50 to 150°C, before and after irradiation.

RB* holes will reduce the fluxes of thermal neutrons on the experiment capsule and its contents. Nevertheless, the specimens will still receive thermal neutron fluences of about 8×10^{25} n/m², resulting in generation of about 0.2 wt % silicon, which will cause about 0.03% swelling. Thus, this type of swelling is small in this case. More importantly, it is independent of temperature. Therefore, the amounts of silicon swelling in

the hot specimen holder and in the relatively cool tube will be the same and will not alter the gas gap. Of course, this conclusion holds only if both holder and tube are made from aluminum. The use of aluminum components in conjunction with non-aluminum components will lead to differential swelling and must be avoided in capsules with small gas gaps subjected to high thermal neutron fluences.

Swelling from voids and from gas bubbles are temperature-dependent in both cases, which means that the amount of swelling from these sources will be different in the hotter holder than in the colder tube. Bubble swelling is due to diffusion and agglomeration of transmutation-produced gases, principally helium and hydrogen, and is most prevalent at temperatures above about half of the absolute melting temperature (T_m) where diffusion is rapid. For aluminum, 0.5 T_m is about 200°C, so this type of swelling might be encountered for all the high-temperature holders but not in the containment tubes, where the temperature is too low. Not enough is known about bubble swelling to allow prediction of the degree of swelling. It is known, however, that such swelling is minimized if bubble coalescence is retarded by trapping the helium on a fine scale at particle-matrix interfaces. Few precipitate particles remain stable in aluminum alloys at 400°C. In 6061-T6 aluminum, for example, the Mg_2Si precipitates responsible for its high strength are dissolved at 400°C. One phase that resists thermal dissipation is aluminum oxide, and aluminum alloys containing finely dispersed flakes of Al_2O_3 have good resistance to radiation damage[12,13,16] and to bubble formation.[16] In addition, they display high-temperature creep resistance.[13] For these reasons, the XAP002 alloy was chosen for the holder and sleeve materials.

Void swelling is associated with an excess of radiation-produced vacancies and is confined to a homologous temperature range of about 0.2 to 0.5 T_m, i.e., below 200°C for aluminum. Therefore, void swelling is possible only in the tube material in these experiments. The excess vacancies are produced largely by fast neutron damage. Swelling in various aluminum alloys irradiated at 55°C is shown in Fig. 9 as a function of fast neutron fluence.[17] This swelling is measured from changes in density; it includes swelling from voids and from transmutation-produced silicon, the latter indicated by the dashed line. Swelling from voids alone is obtained by subtracting the silicon swelling. The fast fluence goal of

ORNL-DWG 81-4415R

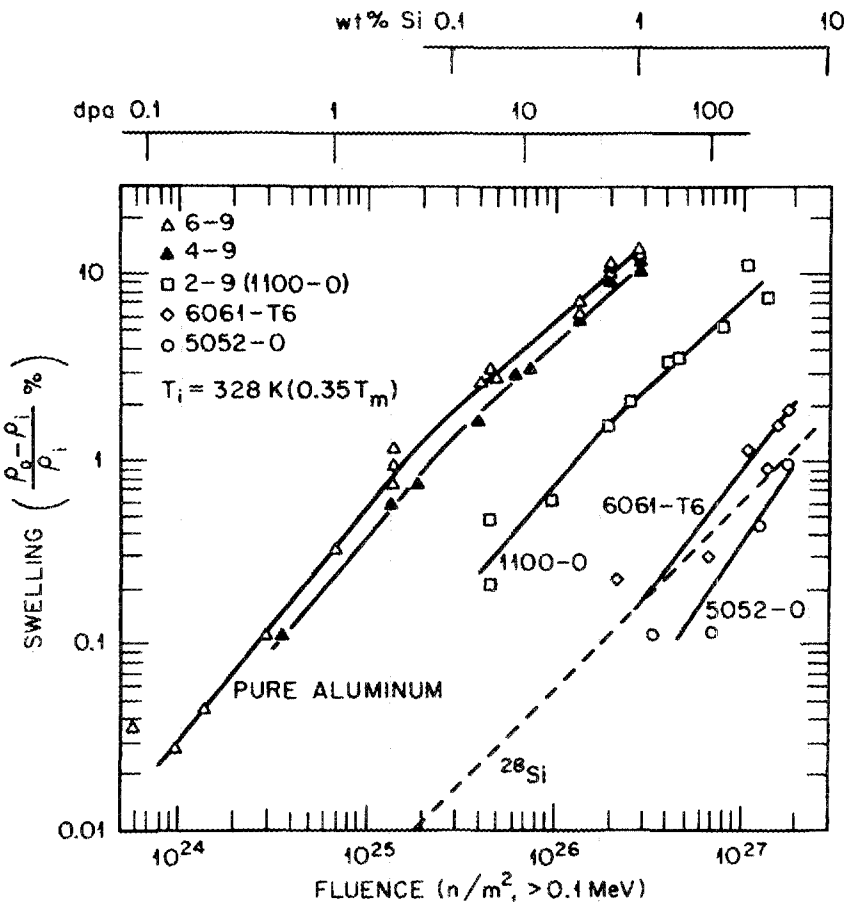

Fig. 9. Swelling in aluminum alloys during neutron irradiation at 55°C.

the U.S.-Japanese experiments is about 2×10^{26} n/m². It is obvious from Fig. 9 that pure aluminum and the 1100 alloys display unacceptedly high void swelling at this fluence. The 6061-T6 and 5052-0 alloys have the greatest resistance to swelling. When their swelling curves are corrected for the effects of silicon, these two alloys show little or no void swelling at the goal fluence.*

The data in Fig. 9 were obtained for irradiations in the HFIR target region and are expected to be representative of unmodified RB positions as well, since the neutron spectra in the two sites are similar. The use of Hf liners in the RB* positions will reduce the contributions from silicon swelling by almost a factor of 10. This will reduce the overall swelling in Fig. 9. Such reductions at the goal fluence will be insignificant except for the 6061 and 5052 alloys.

There are insufficient data to compile a swelling curve for oxide-dispersion alloys of the XAP002 type. However, the few swelling measurements[16] and the large concentrations of stable oxide particles in such alloys, which will trap and recombine point defects, strongly suggest that XAP002-type alloys will have high resistance to void swelling. Therefore, in principle, oxide-dispersion-hardened aluminum alloys would be a near-ideal containment tube material for these irradiations. Unfortunately, commercial production of SAP alloys has ceased, and not enough was on hand to make containment tubes. The 6061-T6 alloy was readily available, and since it is stronger than the 5052-O alloy at the cooling-water temperature and its mechanical properties are less degraded by irradiation,[17] it was selected for the tube material.

Earlier, magnesium and beryllium had been eliminated from further consideration without a full explanation. Now that the effects of swelling on the gas gap have been discussed, the justification for dismissal of these two metals can be presented in better perspective. Magnesium and its alloys are rejected primarily because of uncertainty about their swelling response under irradiation. There are no data for irradiations in contact with cooling water at 55°C or so. Irradiations have been made in sealed capsules where the temperatures are estimated to be 75 to 120°C.[18-20] Under these conditions, pure magnesium swells more than pure aluminum,[18,19] and at high fluences it becomes twisted and distorted because of anisotropic growth in grains of different orientations.[20] Magnesium alloys undergo radiation-assisted phase changes[21] that cause swellings of 0.2 to 0.3% at fast fluences of 2 to 3 $\times$ 10^{26} n/m^2. The propensity for bubble swelling at higher temperatures is expected to be greater in magnesium than in aluminum because the rate of helium production from (n,α) reaction with magnesium is four times larger,[22] and the reaction also produces equal quantitites of neon gas in the magnesium. Beryllium is rejected because, in addition to being brittle, toxic, expensive, and relatively difficult to machine, it displays an unacceptable structural instability under irradiation. Transmutation reactions in beryllium generate large quantitites of insoluble helium and hydrogen isotopes. Accommodation of these gases imposes severe internal stresses, which are relieved in the brittle beryllium by spalling.[23] Maintaining a constant gas gap would be impossible with beryllium.

In summary, certain aluminum alloys offer the best overall properties for support materials for specimens requiring irradiations at temperatures up to 400°C in the RB* positions of the HFIR utilizing nuclear heating and gas gap temperature control. The preferred alloy for the holders and sleeves is the oxide-dispersion-hardened SAP type because of its superior mechanical stability at elevated temperatures and its good resistance to radiation swelling. SAP would also be a good choice for the containment tubes, although 6061-T6 alloy is satisfactory. SAP alloys are currently in short supply, and our reserves for further experiments of the type described herein are inadequate. A potential substitute material has been located, and in the following section a brief assessment of its suitability is described.

EVALUATION OF AN ALTERNATIVE OXIDE-DISPERSION-HARDENED ALUMINUM ALLOY

SAP alloys are no longer manufactured in the United States although there are reports of a resurgence of interest in them and good possibilities of a reintroduction. In the meantime, a West German producer, Sintermetallwerk Krebsöge GMBH, is marketing a product trademarked DISPAL through its U.S. subsidiary.[24] DISPAL materials are very similar to SAP alloys in that they too are mechanically alloyed products made by ball-milling of aluminum powders and consolidation by extrusion. Their manufacturer claims that DISPAL alloys have finer dispersions of oxide and carbide phases and hence better and more reproducible properties. Carbon becomes entrained in both SAP and DISPAL alloys as a residue from organic lubricants used in milling of the aluminum powders. DISPAL alloys are available in a wide range of standard product forms and as custom-made shapes, with oxygen contents in the range 0.4 to 2.5 wt % (0.83 to 5.3 wt % Al_2O_3) and carbon levels in the range 0 to 3 wt %. A technical report on DISPAL alloys[25] shows impressive properties at temperatures up to 500°C. To assess the suitability of DISPAL for use in the U.S.-Japanese MFE experiments, we obtained a piece of extruded DISPAL barstock and evaluated its properties with respect to those of similar bars of two SAP-type alloys, XAP002 and XAP004.

The DISPAL bar was 39 mm diameter and was designated by the manufacturer as DISPAL 0.2. It was specified as having a minimum carbon content of 0.2 wt % and an oxygen content of 1.0 to 1.5 wt %, equivalent to an Al_2O_3 content of 2.1 to 3.2 wt %. Chemical analyses were made by ORNL's Analytical Chemistry Division and are shown in Table 2. The carbon exceeds the specification; the oxygen matches the specified level. The XAP002 and XAP004 alloys were 38-mm-diam barstock received from the archives of a long-defunct ORNL research program. The XAP002 bar was used to provide the holder and sleeve pieces for the 330°C capsule described earlier. These two alloys have specified Al_2O_3 contents of 6 to 8 and 13 to 15 wt %, respectively. Their chemical analyses in Table 2 give values of 9% and 15%.

Flat tensile specimens, 25 mm long with gage sections of 0.75 × 1.5 mm, were machined from the bars of all three alloys in longitudinal and transverse directions. These specimens were tested to failure in vacuum in an Instron machine at temperatures up to 500°C and at a strain rate of 1×10^{-3}/s. The results of these tests are shown in Figs. 10–12. The data for the XAP002 and XAP004 alloys compare very favorably with published tensile data for these materials,[12,13] indicating that the use of miniature tensile specimens in the present tests has not compromised the data. The XAP004 alloy is stronger and less ductile than the XAP002 alloy at all temperatures, as expected from its higher oxide content. The XAP004 alloy is weaker in the transverse direction than in the longitudinal direction, whereas the XAP002 alloy appears to have no directional dependence. Reference data show that both XAP004 and XAP002 are usually weaker in the transverse direction.[13] The DISPAL 0.2, despite its much lower oxide level, displays strength properties in the longitudinal direction equal to those of the XAP002 alloy. In the transverse direction, DISPAL 0.2 has slightly lower ultimate tensile strength (UTS) values but similar yield strengths. The ductility of DISPAL 0.2 is greater than that of XAP002 at temperatures below 300°C in both transverse and longitudinal directions. To test the stability of the DISPAL 0.2 properties, we heat-treated several specimens in air for 24 h at 500°C before the tensile tests. The results are given in Table 3. The heat treatment did not alter the tensile properties significantly.

Table 2. Chemical analyses of test bars

Alloy	Y-12 inspection number	Anal. Chem. Division request no.	wt %							
			Al_2O_3	C	Fe	Si	Cu	Mg	Ti	Al
DISPAL 0.2	16917 (1987)	871209-085 (1986) 33921 (1987)	3.0	0.29	0.04	0.01	0.004	0.004	0.002	Bal
XAP002	16201 (1986)	33777 (1986)	9.0	N.D.[a]	0.32	0.12	0.004	0.013	0.009	Bal
XAP004	16201 (1986)	33777 (1986)	15.0	N.D.[a]	0.32	0.12	0.003	0.017	0.01	Bal

[a]N.D. = Not determined.

ORNL-DWG 88-9301

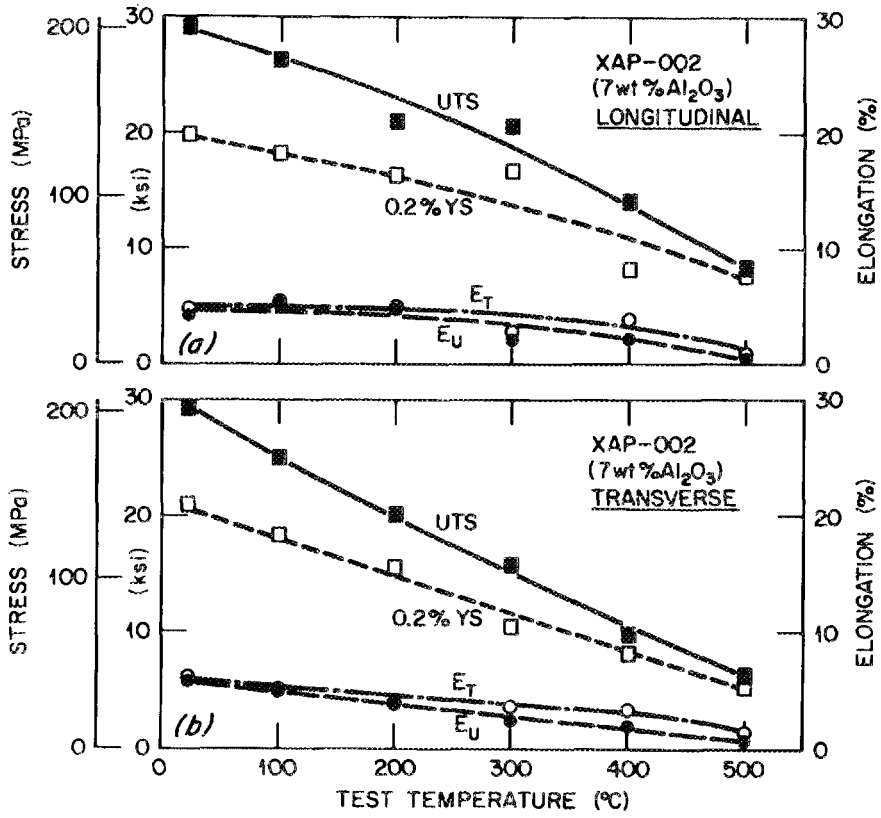

Fig. 10. Temperature dependencies of tensile properties of aluminum alloy XAP002 in longitudinal and transverse directions.

The microstructures of the XAP002 and DISPAL 0.2 alloys were examined by transmission electron microscopy. Examples are presented in Fig. 13. In both cases, the grain sizes were small, 0.5 to 2 μm. The XAP002 contained a larger volume fraction of second-phase particles, many of them being cigar-shaped and up to 0.5 μm long. In the DISPAL 0.2, the entrained particles were generally much smaller, more equiaxed, and more uniformly distributed; many were smaller than about 20 nm. In both alloys, some of the particles existed in relatively large clumps of 0.5 μm or more.

These studies corroborate the manufacturer's claims for DISPAL alloys[25] and demonstrate that the tensile properties of DISPAL 0.2 are similar to those of the XAP002 alloy of higher oxide content. This

ORNL-DWG 88-9297

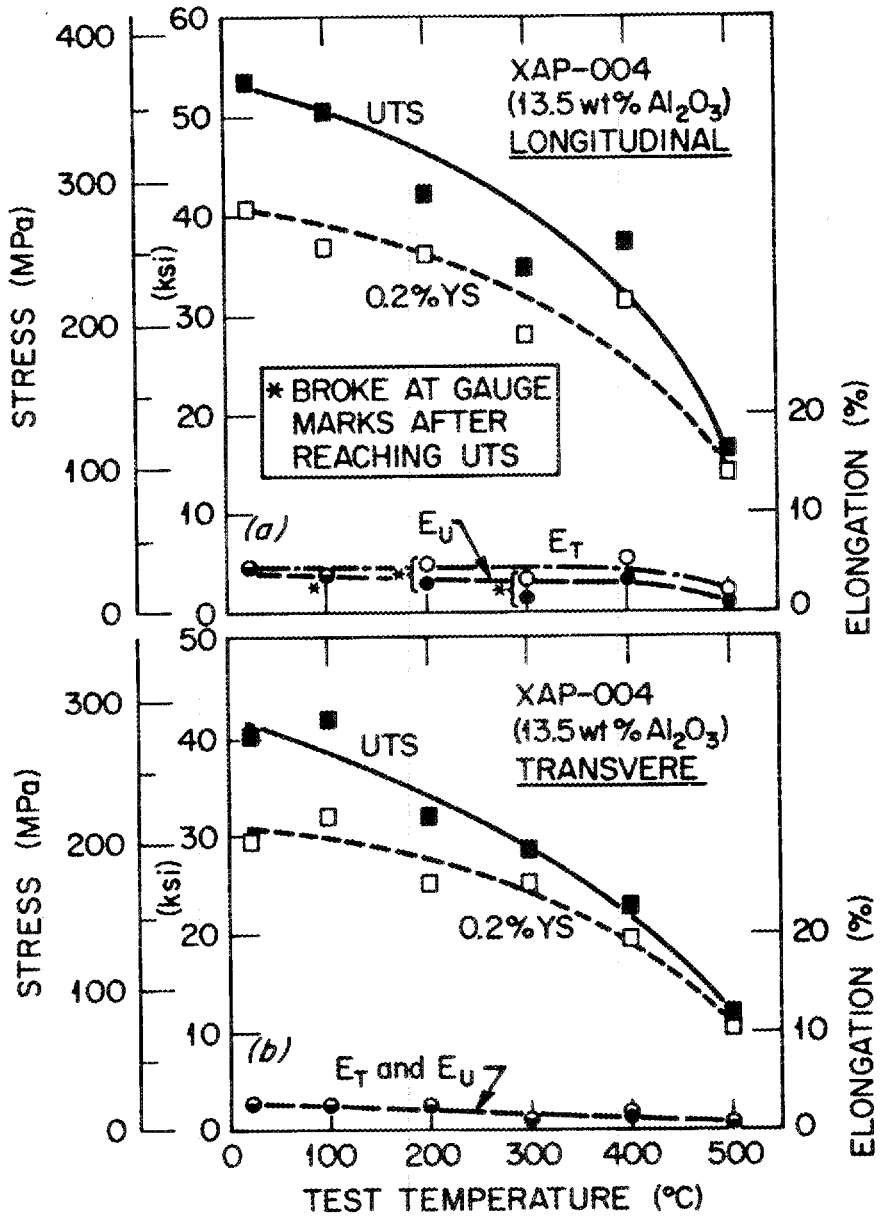

Fig. 11. Temperature dependencies of tensile properties of aluminum alloy XAP004 in longitudinal and transverse directions.

equivalence can be explained by the finer distribution of the dispersed particles in the DISPAL 0.2 alloy. Creep properties were not measured in this evaluation, but given the similarities of the elevated-temperature tensile properties of the DISPAL 0.2 and XAP002 alloys, we expect the

ORNL-DWG 88-9300

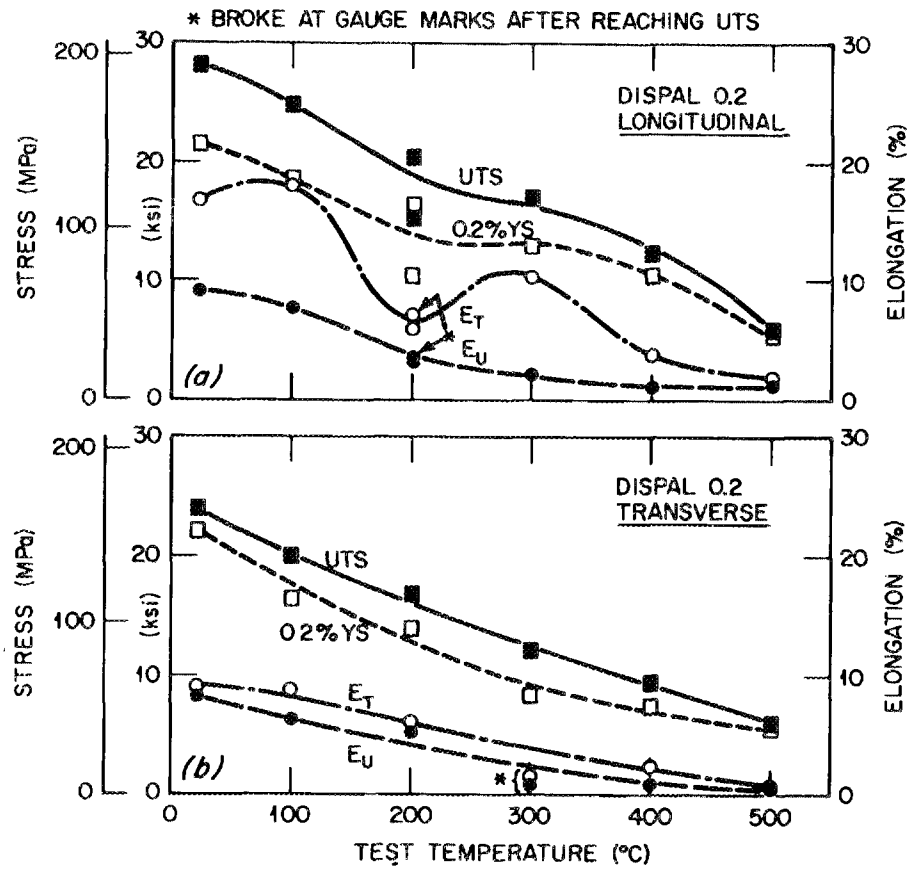

Fig. 12. Temperature dependencies of tensile properties of aluminum alloy DISPAL 0.2 in longitudinal and transverse directions.

creep-rupture properties of the DISPAL 0.2 to be like those of the XAP002-type alloys shown in Fig. 7. These properties are more than adequate for support material applications. Observations made during machining of the alloys indicated that the XAP002 and DISPAL 0.2 gave smooth surfaces, allowing close tolerances to be achieved. The XAP004 alloy gave comparatively rough surfaces, judged less satisfactory for attainment of small gas gaps.

In our opinion, the DISPAL 0.2 alloy should make an acceptable substitute for the XAP002 alloy for use as support structures in the U.S.-Japanese MFE irradiations. An order has been placed for a sufficient quantity of DISPAL 0.2 to satisfy our foreseeable needs.

Table 3. Effects of annealing DISPAL 0.2 for 24 h at 500°C

ID marks	Test temp. (°C)	0.2% Flow stress (MPa)	UTS (MPa)	Total elong. (%)	Uniform elong. (%)	Condition
			Longitudinal			
DL08	22	148.0	194.3	16.6	9.0	No anneal
DL11	22	147.5	190.6	18.0	8.3	Annealed
DL05	300	88.7	117.4	10.1	2.0	No anneal
DL12	300	99.1	112.3	12.5	1.7	Annealed
			Transverse			
DX04	22	153.8	166.9	9.0	8.5	No anneal
DX02	22	114.9	159.3	8.0	7.0	Annealed
DX07	300	56.4	81.4	1.5[a]	0.8[a]	No anneal
DX03	300	69.5	89.9	4.3	2.5	Annealed

[a]Broke at gage mark after reaching UTS.

ORNL-PHOTO 1499-89

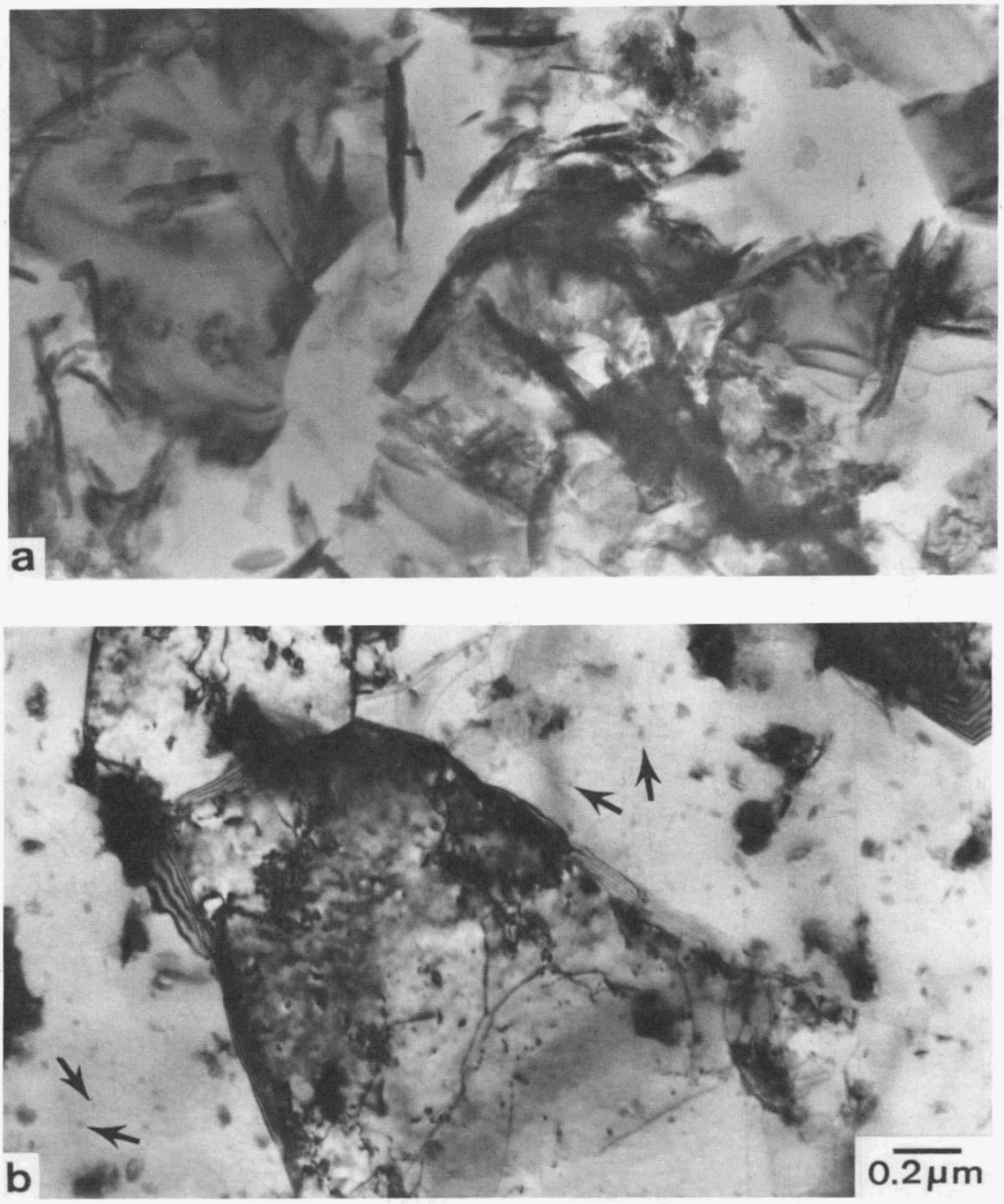

Fig. 13. Typical microstructures of (*a*) XAP002 and (*b*) DISPAL 0.2 alloys, showing finer particles (arrowed) in the DISPAL 0.2 alloy.

ACKNOWLEDGMENTS

The assistance of E. L. Ryan in making the tensile tests and A. M. Williams in preparing the TEM specimens is greatly appreciated. Also, the efforts of J. L. Scott, J. E. Corum, D. L. McElroy, and G. L. Copeland in searching for sources of oxide-dispersion-strengthened aluminum alloys are recognized.

REFERENCES

1. K. R. Thoms et al., *J. Nucl. Mater.* 155–57, 1340–45 (1988).

2. A. W. Longest et al., *J. Nucl. Mater.* 155–57, 1346–49 (1988).

3. Ioan Ursu, *Physics and Technology of Nuclear Materials*, Pergamon Press, Elmsford, N.Y., 1985.

4. C. O. Smith, *Nuclear Reactor Materials*, Addison-Wesley, Reading, Mass., 1967.

5. B. M. Ma, *Nuclear Reactor Materials and Applications*, Van Norstrand Reinhold, New York, 1983.

6. H. Etherington, *Nuclear Engineering Handbook*, McGraw-Hill, New York, 1958, p. 7-66, eq. 5.

7. S. F. Pugh et al., *J. British Nucl. Energy Soc.* 11(4), 313–30, (1972).

8. *Metals Handbook*, 9th ed., Vol. 3, American Society for Metals, Materials Park, Ohio, 1980.

9. *Metals Reference Book*, 5th ed., eds. C. J. Smithells and E. A. Brandes, Butterworths, London and Boston, 1976.

10. G. Piatti and H. A. Weir, *J. Nucl. Mater.* 150, 1–9 (1987).

11. *Materials Handbook for Fusion Energy Systems*, DOE/TIC-10122, U.S. DOE, Office of Fusion Energy, 1980.

12. E. A. Bloch, "Dispersion-Strengthened Aluminum Alloys," *Metall. Rev.* 6(22), 193–239 (1961).

13. *Heavy Water Organic Cooled Reactor—SAP Handbook*, AI-CE-MEMO-24, U.S. Atomic Energy Commission, March 1966.

14. J. S. Benjamin and M. J. Bomford, "Dispersion Strengthened Aluminum Made by Mechanical Alloying," *Metall. Trans.* 8A, 1301–5 (1977).

15. R. T. King, K. Farrell, and A. E. Richt, *Nucl. Metall.* 19, 133–52 (1973).

16. P. J. Maziasz and K. Farrell, *J. Nucl. Mater.* 85–86, 913–17 (1979).

17. K. Farrell, article P11 in *Dimensional Stability and Mechanical Behavior of Irradiated Metals and Alloys*, British Nuclear Energy Society, London, 1983.

18. V. Levy, J. Mathie, A. Risbet, R. Levy, and J. P. Poirier, pp. 63–69 in *Voids Formed by Irradiation of Reactor Materials*, British Nuclear Energy Society, London, 1971.

19. A. Jostsons and K. Farrell, *Rad. Effects* 15, 217–25 (1972).

20. E. F. Sturcken and C. W. Krapp, pp. 996–1017 in *Electron Microscopy and Structure of Materials*, University of California Press, Berkeley, 1972.

21. E. F. Sturcken, *J. Nucl. Mater.* 82, 39–53 (1979).

22. T. A. Gabriel, B. L. Bishop, and F. W. Wiffen, *Calculated Irradiation Response of Materials Using Fission Reactor (HFIR, ORR and EBR-II) Neutron Spectra*, ORNL/TM-6361, Oak Ridge National Laboratory, August 1979.

23. K. Farrell, "Preliminary Metallurgical Examination of Broken Pieces from the HFIR Beryllium Permanent Reflector," letter to J. A. Cox, February 20, 1974, Oak Ridge National Laboratory.

24. Newmet Krebsöge, Route 6 and Burr Road, Terryville, CT 06786: contact Mark Eisenmann.

25. V. Arnhold and J. Baumgarten, "Dispersion-Strengthened Aluminum Extrusions," *Powder Metall. Int.* 12(4), 168–72 (1985).

ORNL/TM-11378
Distribution
Category UC-404

INTERNAL DISTRIBUTION

1-2. Central Research Library
3. Document Reference Section
4-5. Laboratory Records Department
6. Laboratory Records Department, RC
7. ORNL Patent Section
8-10. M&C Records Office
11. D. J. Alexander
12. P. Angelini
13. D. L. Aubuchon
14. C. A. Baldwin
15. R. L. Beatty
16. R. A. Bradley
17. E. D. Clemmer
18. G. L. Copeland
19. J. M. Corum
20. D. F. Craig
21-25. K. Farrell
26. E. C. Fox
27. E. L. Fuller, Jr.
28. M. L. Grossbeck
29. R. W. Hobbs
30. T. Inazuma
31. J. E. Jones Jr.
32. S. Kojima
33-37. A. W. Longest
38. L. K. Mansur
39. D. L. McElroy
40. R. K. Nanstad
41. N. H. Packan
42. R. E. Pawel
43. P. L. Rittenhouse
44. M. Sawai
45. R. L. Senn
46. I. I. Siman-Tov
47. G. M. Slaughter
48. J. O. Stiegler
49. R. E. Stoller
50. F. W. Wiffen
51. T. Zacharia
52. A. D. Brailsford (Consultant)
53. H. D. Brody (Consultant)
54. D. P. Pope (Consultant)
55. M. L. Savitz (Consultant)
56. E. R. Thompson (Consultant)
57. J. B. Wachtman (Consultant)

EXTERNAL DISTRIBUTION

58. Department of Fuels and Materials Research, Japan Atomic Energy Research Institute, Tokai-mura, Ibaraki-ken, 319-11, Japan

59. M. Eisenmann, Newmet Krebsöge, Route 6 and Burr Road, Terryville, CT 06786

60. DOE, Division of Magnetic Fusion Energy, Washington, DC 20545

    T. C. Reuther (ER-533, J224/GTN)

61-63. DOE, Division of Materials Sciences, Washington, DC 20545

    J. B. Darby (ER-131, J321/GTN)
    R. J. Gottschall (ER-131, J321/GTN)
    I. L. Thomas (ER-132, J321/GTN)

64. DOE, Office of Fossil Energy, Washington, DC 20545

    M. I. Singer (FE-14, B115/GTN)

65. DOE, Oak Ridge Operations Office, P.O. Box 2001, Oak Ridge, TN 37831-8600

    Office of Assistant Manager for Energy Research and Development

66-110. DOE, Office of Scientific and Technical Information, P.O. Box 62, Oak Ridge, TN 37831

For distribution as shown in DOE/OSTI-4500, Distribution Category UC-404 (Materials).